Journal of Translational Medicine

RESEARCH

Open Access

An novel effective and safe model for the diagnosis of nonalcoholic fatty liver disease in China: gene excavations, clinical validations, and mechanism elucidation

Jida Wang[1], Beitian Jia[1], Jing Miao[1], Dun Li[1], Yin Wang[1], Lu Han[1], Yin Yuan[1], Yuan Zhang[4], Yiyang Wang[1], Liying Guo[2], Jianwei Jia[2], Fang Zheng[1], Sizhen Lai[1], Kaijun Niu[3], Weidong Li[5], Yuhong Bian[1*] and Yaogang Wang[1,3,4*]

Abstract

Background Non-alcoholic fatty liver disease (NAFLD) is one of the most common chronic liver diseases. NAFLD leads to liver fibrosis and hepatocellular carcinoma, and it also has systemic effects associated with metabolic diseases, cardiovascular diseases, chronic kidney disease, and malignant tumors. Therefore, it is important to diagnose NAFLD early to prevent these adverse effects.

Methods The GSE89632 dataset was downloaded from the Gene Expression Omnibus database, and then the optimal genes were screened from the data cohort using lasso and Support Vector Machine Recursive Feature Elimination (SVM-RFE). The ROC values of the optimal genes for the diagnosis of NAFLD were calculated. The relationship between optimal genes and immune cells was determined using the DECONVOLUTION algorithm CIBERSORT. Finally, the specificity and sensitivity of the diagnostic genes were verified by detecting the expression of the diagnostic genes in blood samples from 320 NAFLD patients and liver samples from 12 mice.

Results Through machine learning we identified *FOSB*, *GPAT3*, *RGCC* and *RNF43* were the key diagnostic genes for NAFLD, and they were further demonstrated by a receiver operating characteristic curve analysis. We found that the combined diagnosis of the four genes identified NAFLD samples well from normal samples (AUC = 0.997). *FOSB*, *GPAT3*, *RGCC* and *RNF43* were strongly associated with immune cell infiltration. We also experimentally examined the expression of these genes in NAFLD patients and NAFLD mice, and the results showed that these genes are highly specific and sensitive.

Conclusions Data from both clinical and animal studies demonstrate the high sensitivity, specificity and safety of FOSB, GPAT3, RGCC and RNF43 for the diagnosis of NAFLD. The relationship between diagnostic key genes and immune cell infiltration may help to understand the development of NAFLD. The study was reviewed and approved by Ethics Committee of Tianjin Second People's Hospital in 2021 (ChiCTR1900024415).

*Correspondence:
Yuhong Bian
Bianyuhong_2012@163.com
Yaogang Wang
YaogangWANG@tmu.edu.cn

Full list of author information is available at the end of the article

Keywords Nonalcoholic fatty liver disease, Machine learning, Biomarkers

Introduction

Non-alcoholic fatty liver disease (NAFLD) is one of the most common chronic liver diseases, that affects one in four adults worldwide [1]. The current global prevalence of NAFLD is about 25.2% and is expected to reach 33.5% by 2030 [2]. At the beginning of the 21st century, the prevalence of NAFLD in China was estimated to be 23.8% (95% CI: 16.4-31.2%). In 2018, the NAFLD prevalence reached 32.9% (95% CI: 28.9-36.8%). By 2030, the total number of NAFLD patients in China is expected to increase up to 314.58 million and is expected to reach 50.8%, making it the fastest-growing country in the world in terms of NAFLD prevalence [3].

NAFLD is a clinicopathological syndrome characterized by diffuse bullae of fat in hepatocytes [4]. The inflammatory subtype of NAFLD is nonalcoholic steatohepatitis (NASH), which can progress to cirrhosis and even hepatocellular carcinoma [5]. NAFLD is a risk factor for chronic kidney disease [6], cardiovascular disease [7], and sleep apnea [8]. In addition to that, NAFLD may remain silent for several years before the manifestation of its representative symptoms and structural changes become visible in a radiography [9]. Therefore, early diagnosis of NAFLD is essential to delay the progression of the disease and for the treatment [10].

Unfortunately, there is still a lack of such early diagnostic tools in clinical practice [11]. At present, liver biopsy remains the gold standard for NAFLD diagnosis, despite the limitations regarding sampling variability, invasivity, and high cost. Early detection of hepatic steatosis is the first step in the diagnosis of NAFLD [12], and noninvasive assessment models such as the fatty liver index and the hepatic steatosis index are the initial strategies suitable for use in primary care hospitals as a screen for hepatic steatosis [13]; in terms of imaging, ultrasound, although widely available, has a low sensitivity for mild hepatic steatosis, and therefore is not recommended as a tool for screening for hepatic steatosis in the AASLD guidelines [14, 15]. Controlled attenuation parameters allow for immediate semiquantitative assessment and are gradually becoming more widely used, whereas the proton density fat fraction of MRI is the most accurate, reproducible, and precise means of quantifying hepatic steatosis, but is now used only for clinical research due to cost and patient acceptance [16]. Therefore, the development of new diagnostic biomarkers that can reflect the entity of liver injury is critical for early diagnosis and treatment of NAFLD [17, 18].

With the development of high-throughput gene microarray technology, researchers can analyze the gene and mRNA differences among samples derived from patients with a variety of diseases and from healthy humans [19]. Many specific genes involved in the progression of NAFLD have been already identified. For example, the expression level of fibroblast growth factor 21 (FGF21) in the liver of NAFLD patients is considerably lower than that of healthy individuals [20]. In a mouse model, FGF21 was associated with a decrease in the progression of NAFLD [21]. Moreover, the interference of the FGF21–mechanistic target of rapamycin complex 1 axis reduces chronic NAFLD via stimulation of FGF21 kinase, suggesting that the FGF21 pathway may be a potential therapeutic target for NAFLD [22]. Additionally, *Xie et al.*. found downregulated the expression of FK506-binding protein 38 (FKBP38) in the livers of NAFLD patients when compared with healthy livers. Furthermore [23], FKBP38 overexpression enhances the mitochondrial fatty acid oxidation defense and promotes adipose oxidation in fat cells through the mTOR/SREBPs signaling pathway [24]. These findings suggest an important role for some functional genes in NAFLD progression. However, whether these functional genes can be used for the diagnosis of NAFLD remains unclear.

In the present study, we aimed to identify novel NAFLD diagnostic genes by using bioinformatics and machine learning. A Gene Expression Omnibus (GEO) dataset (GSE89632) was used to screen differentially expressed genes (DEGs) between NAFLD and healthy specimens. Next, machine learning was used to analyze the diagnostic value of these genes in NAFLD. The expression of these genes was further examined in NAFLD animal model mice liver and clinical patients blood. We also examined the expression of these genes in hepatitis B, hepatitis C, and autoimmune hepatitis (AID) patients blood to determine their specificity.

Materials and methods

Microarray data

The microarray data used to establish the diagnostic model for NAFLD were the GSE89632 mRNA expression profile data (including blood samples from 19 NAFLD patients and 24 normal controls), was downloaded from GEO (https://www.ncbi.nlm.nih.gov/geo/) [25]. Screening criteria: the period of data collection was before January 2023. The dataset intelligently contained healthy people and patients with NAFLD (excluding patients with alcoholic fatty liver disease, hepatitis, liver fibrosis, and hepatocellular carcinoma). The patients with fatty liver disease had not been subjected to pharmacological interventions as at the time of data collection.

Identification of DEGs

DEGs between NAFLD and normal samples were identified using R software with the Limma package. The thresholds for DEGs were set as $|Log_2FC|>1$ and false discovery rate (FDR) < 0.05.

Functional enrichment analyses

Gene Ontology (GO) and Kyoto Encyclopedia of Genes and Genomes (KEGG) pathway analysis were performed using "clusterProfiler" in the R software to complete the analysis of patients in the high-risk and low-risk groups. GO terms and KEGG pathways with $P<0.05$ were considered statistically significant. Disease Ontology enrichment analysis was performed using the "clusterProfiler" and "DOSE" packages in the R software.

Identification of candidate diagnostic markers

Two machine learning algorithms, lasso and support vector machine recursive feature elimination (SVM-RFE), were used to predict the NAFLD status using possible diagnostic factors. The lasso regression algorithm was performed to identify genes significantly associated with the discriminative power of NAFLD and healthy specimens using R software with the "GlMNet" package. Support vector machine (SVM) is a monitored machine learning algorithm that is widely used for both classification and regression analyses. Moreover, the recursive feature elimination (RFE) algorithm is used to avoid overfitting and thus screen the optimal genes from the metadata queue. Therefore, to identify the gene set with the strongest recognition ability, SVM-RFE was used to screen suitable features [26].

CIBERSORT analysis

The deconvolution algorithm CIBERSORT (http://cibersort.stanford.edu/) was used to analyze the cell composition of complex tissue samples according to the gene expression profile of each cell type. With the help of the CIBERSORT algorithm, we identified the immune responses of 22 immune cell types and determined their relationships with the mRNA levels of key genes in normal and NAFLD samples. The purpose of this study was mainly to determine the link between these immune cells.

Clinical specimens

Blood samples were collected from patients with NAFLD ($n=320$, including 160 females and 160 males, with the age of 21–59 years), Hepatitis B($n=289$, including 145 females and 144 males, with the age of 21–59 years), Hepatitis C ($n=292$, including 152 females and 140 males, with the age of 21–59 years) or AID ($n=289$ per group, including 156 females and 133 males, with the age of 21–59 years) who were diagnosed according to the criteria released by the Chinese Society of Hepatology Medical Association (Table 1). Patients with hepatitis B and hepatitis C were simply infected with the virus and are not in the active phase, but have the same AST and ALT abnormalities as patients with NAFLD. Healthy blood samples were obtained from patients without any disease ($n=300$, including 150 females and 150 males, with the age of 21–59 years). Informed consent was obtained from all cases for tissue sample use. The present work gained approval from Ethics Committee of Tianjin Second People's Hospital.

Animal specimens

Twelve 8-week-old specific-pathogen-free male C57BL/6 mice weighing about 20 g were maintained under a 12-h light/dark cycle with a temperature of 22±2 °C and a humidity of 50±5% with free access to food and water. All animal procedures were approved by the Institutional Anima·l Care and Use Committee of the Tianjin University of Chinese Medicine. The mice were adaptively fed for seven days before the experiments and were then randomly divided into two groups: normal (fed with standard chow for 12 weeks) and NAFLD model (fed with a NAFLD/NASH high-fat-rich diet and drinking water containing fructose for 12 weeks) groups. After 12 weeks, the mice were sacrificed, and their liver samples were collected.

Real-time polymerase chain reaction (RT-PCR) assay

Total RNA was extracted from the liver samples by TRIzol (Invitrogen), according to the manufacturer's protocol. cDNA was first synthesized using the extracted RNA with random primers and a reverse transcription kit (Takara, China). The reverse transcription process was performed as follows: 37 °C for 15 min followed by 5s at 85 °C. Then qRT-PCR was carried out using a Power

Table 1 Patient demographics and biochemical index information

Classification	F/ M	AST	ALT	TG	TC	LDL-c	virus	Brightness mode
Control	150/150	25.83 ± 5.87	18.81 ± 4.66	1.62 ± 0.21	3.89 ± 0.54	2.64 ± 0.41	-	negative
NAFLD	160/160	92.81 ± 9.3**	136.5 ± 60.7*	2.56 ± 0.52*	6.94 ± 0.83*	4.03 ± 0.19*	-	positive
Hepatitis B	145/144	50.5 ± 8.18*	33 ± 14.3**	1.42 ± 0.8	3.79 ± 0.28	2.87 ± 1.06	+	negative
Hepatitis C	152/140	52.83 ± 17.6*	67.66 ± 2.7*	1.89 ± 0.56	4.01 ± 1.48	3.05 ± 0.84	+	negative
ALD	156/133	48.5 ± 2.18*	46.5 ± 21.7*	2.87 ± 0.42*	5.23 ± 0.76*	3.98 ± 0.77**	-	positive

Compared with the Control, NAFLD, MG Hepatitis B, Hepatitis C and ALD *$P<0.05$, **$P<0.01$

SYBR Green kit (Takara, China) on an ABI 7500 instrument. The relative mRNA level was calculated using the $2^{-\Delta\Delta Ct}$ method. Glyceraldehyde-3-phosphate dehydrogenase (*GAPDH*) was used as an internal control for data normalization. The primers for the genes encoding an AP-1 transcription factor subunit (*FOSB*), glycerol-3-phosphate acyltransferase 3 (*GPAT3*), regulator of the cell cycle (*RGCC*), and ring finger protein 43 (*RNF43*) as well as *GAPDH* are shown in Table 2.

Statistical analysis

The Student's *t* test was used to compare the gene expression between NAFLD tissues and adjacent tissues. To test the classification effect of key genes on NAFLD and healthy samples, the "pROC" package in R software was used to calculate the receiver operating characteristic (ROC) curve and the area under the curve (AUC). Statistical analyses were performed using R software (Version 3.5.3) and Prism (GraphPad Prism, USA). A *P*-value of <0.05 was considered statistically significant.

Results

Identification of DEGs in NAFLD

Firstly, we find the differentially up-regulated or down-regulated genes in the NAFLD samples in the dataset. The data of 19 NAFLD cases and 24 controls from the GEO dataset (GSE89632) were included for analysis. After the batch effect was removed, the DEGs of the metadata were analyzed by R software with the Limma package. We identified 334 DEGs, including 223 upregulated genes and 111 downregulated genes (Fig. 1A).

Table 2 Primer sequences to measure mRNA levels using quantitative RT-PCR

Gene (Mus musculus)	Primer	Sequence (5′–3′)
FOSB (mouse)	forward	CCTCCGCCGAGTCTCAGTA
	reverse	CCTGGCATGTCATAAGGGTCA
GPAT3 (mouse)	forward	CGGATTATCCCTGGGTATCTCG
	reverse	CGAAGTCCCTTCCTCGAAGAC
RGCC (mouse)	forward	GAGCGCCACTTCCACTATGAG
	reverse	GGAGAGGAGTTGGTTGGAGAA
RNF43 (mouse)	forward	CACGAGTTTCATCGAACGTGT
	reverse	CTGGCGAATGAGGTGGAGT
GAPDH (mouse)	forward	AGGTCGGTGTGAACGGATTTG
	reverse	GGGGTCGTTGATGGCAACA
FOSB (human)	forward	GCTGCAAGATCCCCTACGAAG
	reverse	ACGAAGAAGTGTACGAAGGGTT
GPAT3 (human)	forward	CGCTGGTTCTCGGCTTCAT
	reverse	TGGCCCACTCTAAAGTTTTCAC
RGCC (human)	forward	CGCCACTTCCACTACGAGG
	reverse	CAGCAATGAAGGCTTCTAGCTC
RNF43 (human)	forward	CATCAGCATCGTCAAGCTGGA
	reverse	TTACCCCAGATCAACACCACT
GAPDH (human)	forward	GGAGCGAGATCCCTCCAAAAT
	reverse	GGCTGTTGTCATACTTCTCATGG

Functional enrichment analyses

Next, GO and KEGG analyses were performed for these 334 DEGs using R software with the Cluster Profile package. The results showed that the 334 DEGs mainly participated in the response to chemicals, negative regulation of cellular processes, response to organic substances, cellular response to chemical stimuli, response to external stimuli, cell death, programmed cell death, signaling receptor binding, sequence-specific DNA binding, transcription regulatory region DNA binding, the plasma membrane part, the intrinsic component of the plasma membrane, and the integral component of the plasma membrane (Fig. 1B–D). Meanwhile, KEGG analysis showed that the following pathways were significantly enriched: cytokine–cytokine receptor interactions, the interleukin (IL)-17 signaling pathway, the tumor necrosis factor (TNF) signaling pathway, and transcriptional dysregulation in cancer (Fig. 1E).

Identification of diagnostic marker candidates

Two different algorithms were used to identify potential biomarkers. SVM-RFE algorithm and lasso regression algorithm are the core independent variables in screening differential genes, which can reflect the characteristics of the disease. These DEGs were analyzed by the lasso regression algorithm, which determined 12 genes as diagnostic markers for NAFLD (Fig. 2A). Through the SVM-RFE algorithm (Fig. 2B), a subset of eight genes was determined using the difference analysis object. Finally, four overlapping genes (*FOSB*, *GPAT3*, *RNF43*, and *RGCC*) were identified with the two algorithms (Fig. 2C). These four genes (*FOSB*, *GPAT3*, *RNF43*, and *RGCC*) may be the key genes involved in the progression of NAFLD.

The expression and diagnostic value of FOSB, GPAT3, RNF43, and RGCC in NAFLD

Compared with the healthy samples, the expression levels of *FOSB*, *GPAT3*, and *RGCC* were significantly downregulated in the NAFLD samples (Fig. 2D, E, F); whereas the expression level of *RNF43* was significantly upregulated in the NAFLD samples (Fig. 2G). Next, ROC curve analysis was performed to evaluate the diagnostic value of *FOSB*, *GPAT3*, *RGCC*, and *RNF43*. We found that the AUCs of *FOSB* (Fig. 2H), *GPAT3* (Fig. 2I), *RGCC* (Fig. 2J), and *RNF43* (Fig. 2K) were 0.974, 0.983, 0.985, and 0.958, respectively, suggesting that all four genes showed a strong ability to differentiate NAFLD samples from normal samples.

Then, ROC curve was used to analyze the diagnostic value of combined two, three and four genes for NAFLD. We found that two, three and four genes exhibited a

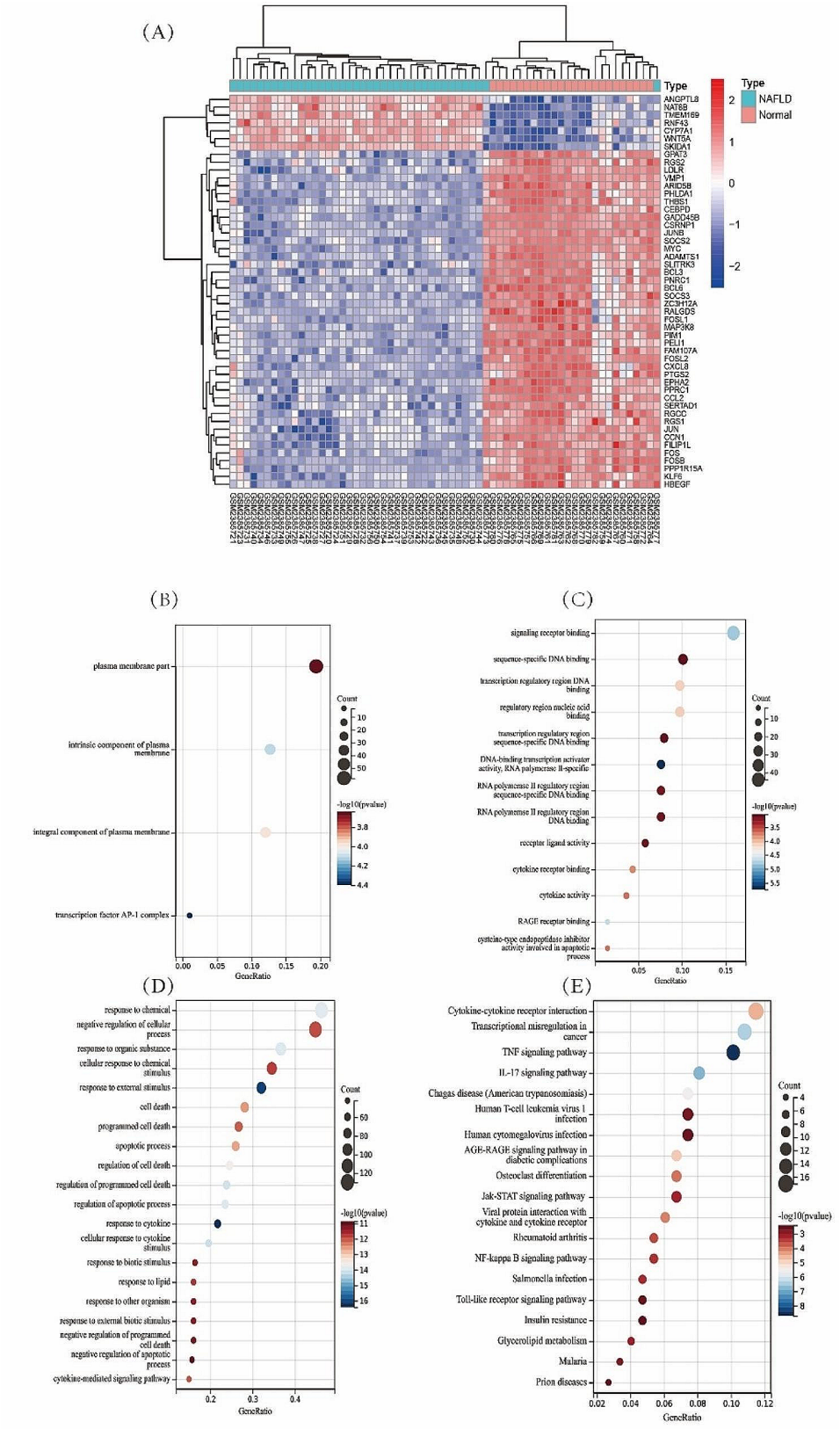

Fig. 1 **A**: DEGs between NAFLD and healthy specimens. GO analysis (**B**: cellular components, **C**: molecular functions, **D**: biological processes) and KEGG analysis (**E**) of 334 DEGs via the ClusterProfile package of R software

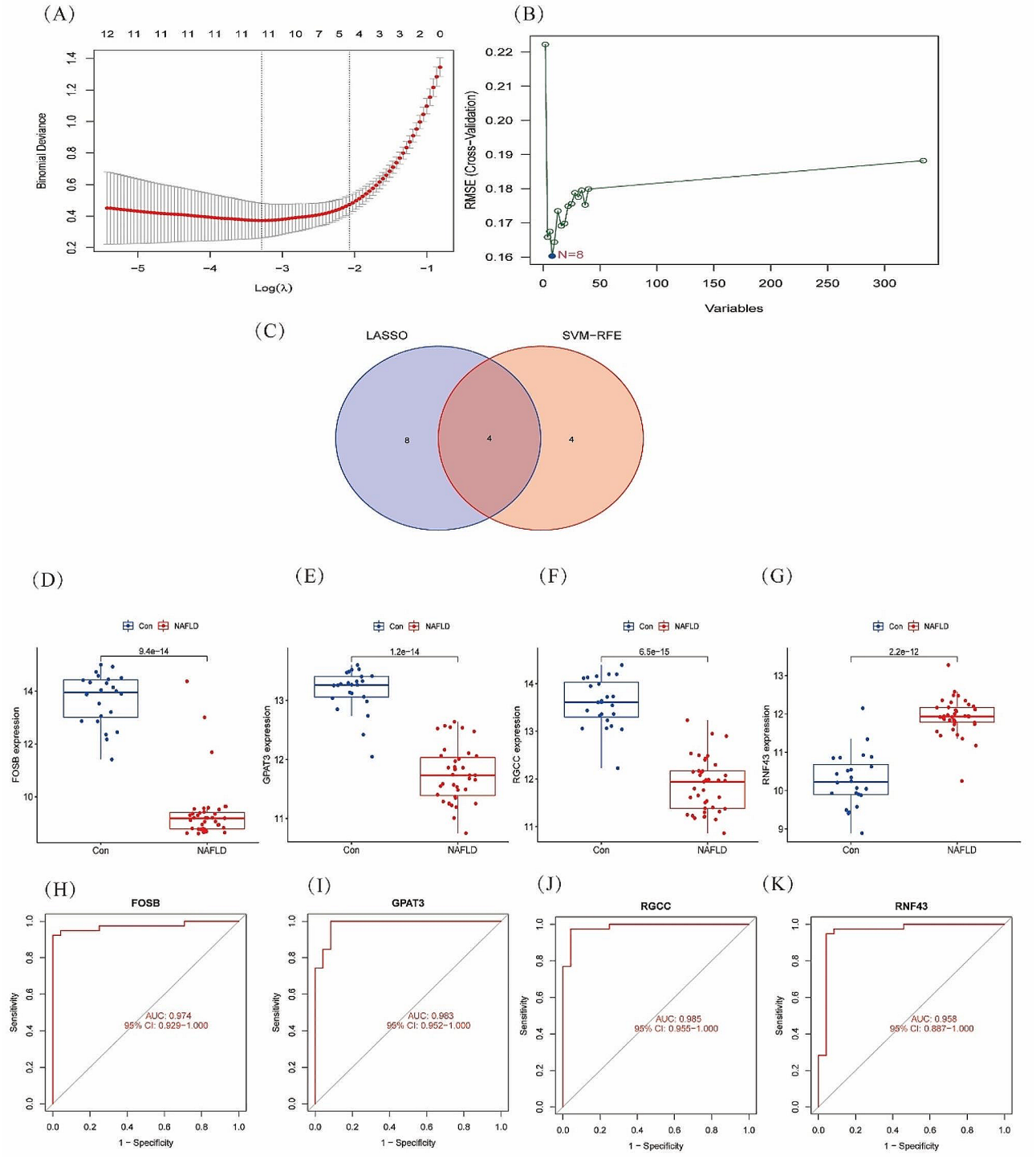

Fig. 2 Identification of the gene candidates for NAFLD diagnosis: (**A**) tuning feature selection using the lasso model; (**B**) the screening of gene candidates by the SVM-RFE algorithm; (**C**) The Venn diagram presenting for gene candidates shared by lasso and SVM-RFE. Expression of *FOSB*(**D**), *GPAT3*(**E**), *RGCC*(**F**), and *RNF43*(**G**) in the common human and NAFLD in the dataset. Expression of *FOSB*(**H**), *GPAT3*(**I**), *RGCC*(**G**), and *RNF43*(**K**) in the common human and NAFLD in the dataset

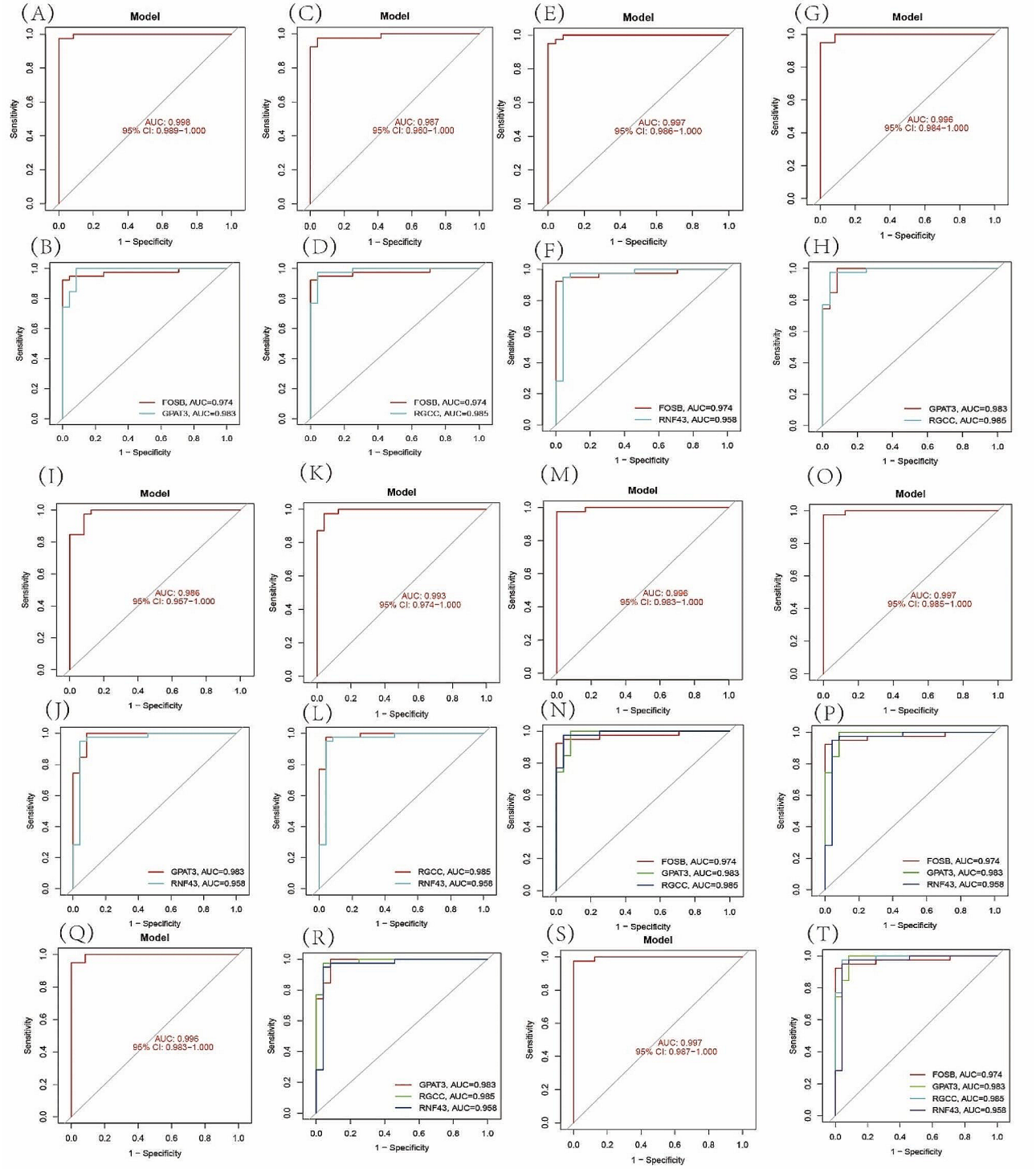

Fig. 3 The ROCs of two, three and four genes. (**A** - **L**) The ROCs of combined two genes. (**N** - **R**) The ROCs of combined three genes. (**S** - **T**) The ROCs of combined four genes

strong ability in screening NAFLD samples from normal samples (Fig. 3A, B AUC=0.998; C, D AUC=0.997; E, F AUC=0.997; G, H AUC=AUC=0.996; I, J AUC=0.986; K, L AUC=AUC=0.993; M, N AUC=0.996; O, P AUC=AUC=0.997; Q, R AUC=0.996; S, T AUC=0.997;) Each gene alone was used to diagnose NAFLD at a very high level, and the combination of all four genes had the highest ROC value for the diagnosis of NAFLD.

FOSB, GPAT3, RGCC, and RNF43 are associated with the infiltration levels of immune cells

Immune cell infiltration in the tumor microenvironment is an independent predictor of overall survival and prognosis. Therefore, we investigated the coefficients of *FOSB*, *GPAT3*, *RGCC*, and *RNF43* and the infiltration status of immune cells in NAFLD and normal samples to determine the correlation between them. The CIBERSORT method was used to analyze the characteristics of immune cells. The composition of the immune cells in NAFLD and normal specimens as well as the relationships between immune cells are presented in Fig. 4A–B. The levels of $CD8^+$ T cells, resting dendritic cells were significantly different between the normal and NAFLD samples (Fig. 4C).

Next, the relationships between the expression levels of *FOSB*, *GPAT3*, *RGCC*, and *RNF43* and the infiltration levels of immune cells were explored. *FOSB* was positively correlated with activated mast cells, monocytes, neutrophils (Fig. 5), (A. Mast cells resting), (B. T cells gamma delta), (C. Macrophages M2), (D. T cells CD4 memory activated), (E. Dendritic cells resting), (F. T cells CD8), (G. Dendritic cells activated), (H. B cells naive), (I. Monocytes), (J. T cells follicular helper), (K. Neutrophils), (L. Mast cells activated). Meanwhile, *GPAT3* was positively correlated with activated mast cells, neutrophils (Fig. 6), (A. Mast cells resting), (B. Neutrophils), (C. Monocytes), (D. Dendritic cells activated), (E. B cells naive), (F. Mast cells activated), (G. T cells gamma delta), (H. Macrophages M2), (I. Dendritic cells resting), (J. T cells CD8). Moreover, *RGCC* was positively correlated with activated mast cells, neutrophils, monocytes, activated dendritic cells, naive B cells, plasma cells, while negatively associated with memory B cells, resting dendritic cells (Fig. 7), (A. Monocytes), (B. Neutrophils), (C. B cells naive), (D. Plasma cells), (E. Dendritic cells activated), (F. Mast cells activated), (G. B cells memory), (H. T cells CD8), (I. Mast cells resting), (J. T cells CD4 memory activated), (K. T cells gamma delta), (L. Macrophages M2), (M. Dendritic cells resting). Finally, *RNF43* was positively correlated with γδ T cells, M2 macrophages (Fig. 8), (A. Mast cells resting), (B. Macrophages M2), (C. Dendritic cells resting), (D. T cells gamma delta), (E. T cells CD8), (F. Mast cells activated), (G. Dendritic cells activated), (H. B cells naive), (I. Monocytes), (J. Neutrophils). These data suggest that *FOSB*, *GPAT3*, *RGCC*, and *RNF43* may be involved in the progression of NAFLD by modulating some types of immune cells.

Validation of the expression of four diagnostic genes

RT-PCR was used to validate the expression of *FOSB*, *GPAT3*, *RGCC*, and *RNF43* in the livers of NAFLD model mice. Compared with the normal mice, the expression levels of *FOSB*, *GPAT3*, and *RGCC* were significantly reduced (Fig. 9A, B and C), while the expression level of *RNF43* was significantly increased (Fig. 9D) in the NAFLD mice. We further confirmed the mRNA expression of these four genes in the blood of NAFLD patients (Fig. 9E-H). The data showed similar changes as in mice. These results further suggest that *FOSB*, *GPAT3*, *RGCC*, and *RNF43* may be potential diagnostic biomarkers of NAFLD.

We also detected the expression of *FOSB*, *GPAT3*, *RGCC*, and *RNF43* in the blood of patients with hepatitis B (Fig. 9I-L), hepatitis C (Fig. 10A-D) and AIH (Fig. 9E-F). Compared with the healthy people, the expression levels of *GPAT3* was significantly reduced (Fig. 9J), while the expression level of *FOSB*, *RGCC*, and *RNF43* showed no significant change (Fig. 9I, K, L) in patients with hepatitis B; the expression levels of *RNF43* was significantly increased (Fig. 10D), while the expression level of *FOSB*, *RGCC*, and *GPAT3* showed no significant change (Fig. 9A, B, C) in patients with hepatitis C; the expression level of *RGCC* was significantly reduced (Fig. 9G), while the expression level of *RNF43* was significant increased (Fig. 9H) in the AIH patients. These results further suggest that combine *FOSB*, *GPAT3*, *RGCC*, and *RNF43* may be potential diagnostic biomarkers of NAFLD.

Discussion

NAFLD is the most common type of liver disease that affects many individuals worldwide [27]. Hepatitis, cirrhosis and liver cancer caused by NAFLD are global public health problems [3, 28–31]. The prevalence of NAFLD in our population is increasing annually, and the proportion of new cases of NAFLD is about 4% each year [32]. There is a significant difference in the prevalence rate of NAFLD in different regions, with the prevalence rate in the economically developed eastern and southern regions being higher than that in the central and western inland regions. The difference in lifestyles could also an important reason for the difference in prevalence rates [33]. Over the past two decades, the burden of NAFLD has increased significantly with China's booming economy and radical lifestyle changes. The early diagnosis of NAFLD is essential for the treatment of this disease, Unfortunately, there are no diagnostic tools that can allow a prompt diagnosis [34, 35].

In our study, machine learning methods were used to find DEGs. We analyzed the GEO dataset and identified 334 DEGs between NAFLD and healthy samples. GO analysis showed that these 334 DEGs were mainly involved in chemical reactions, negative regulation of cell processes, organic material and cell-to-chemical stimulation reactions. KEGG pathway analysis showed that cytokine–cytokine receptor interactions, the interleukin (IL)-17 signaling pathway, the tumor necrosis factor (TNF) signaling pathway, and transcriptional

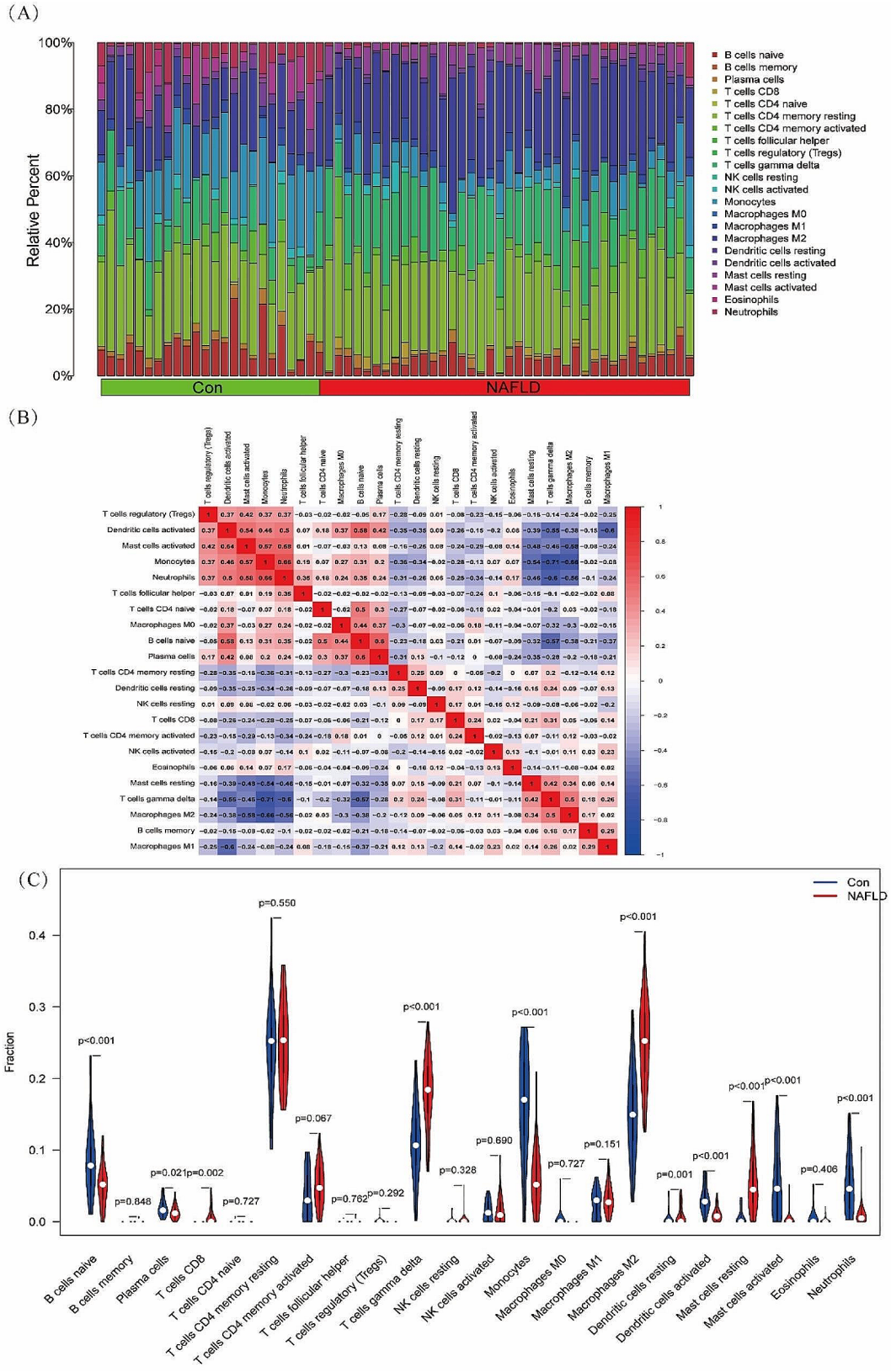

Fig. 4 Relationship between four genes (FOSB, GPAT3, RGCC and RNF43) and infiltration levels of immune cells. (**A**, **B**) The percentage of the 22 immunocytes identified using CIBERSORT. (**C**) The differences in the composition of immunocytes between healthy and NAFLD samples

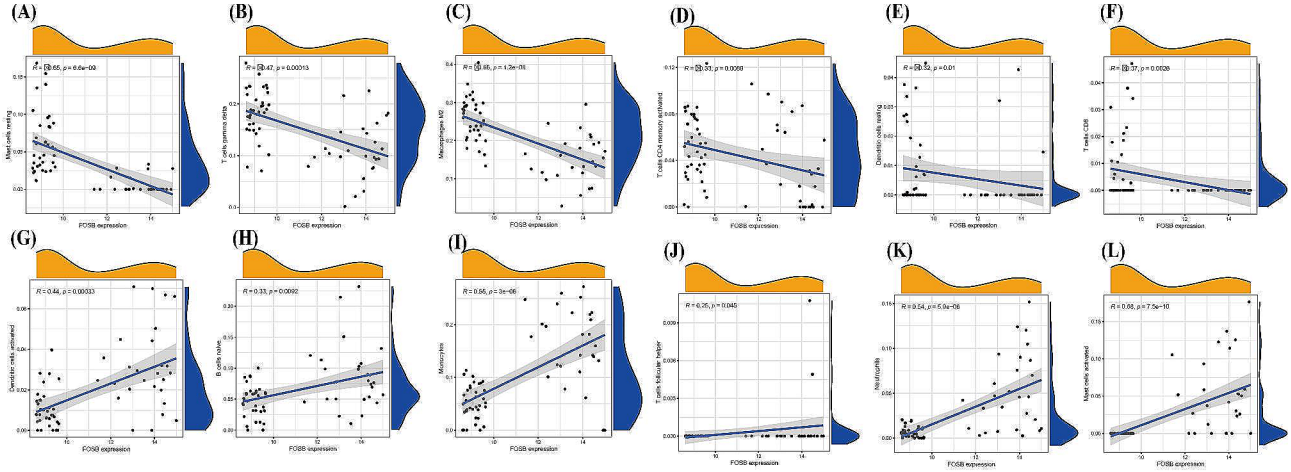

Fig. 5 Correlation between FOSB and infiltrating immune cells in NAFLD and healthy samples. (A. Mast cells resting), (B. T cells gamma delta), (C. Macrophages M2), (D. T cells CD4 memory activated), (E. Dendritic cells resting), (F. T cells CD8), (G. Dendritic cells activated), (H. B cells naive), (I. Monocytes), (J. T cells follicular helper), (K. Neutrophils), (L. Mast cells activated)

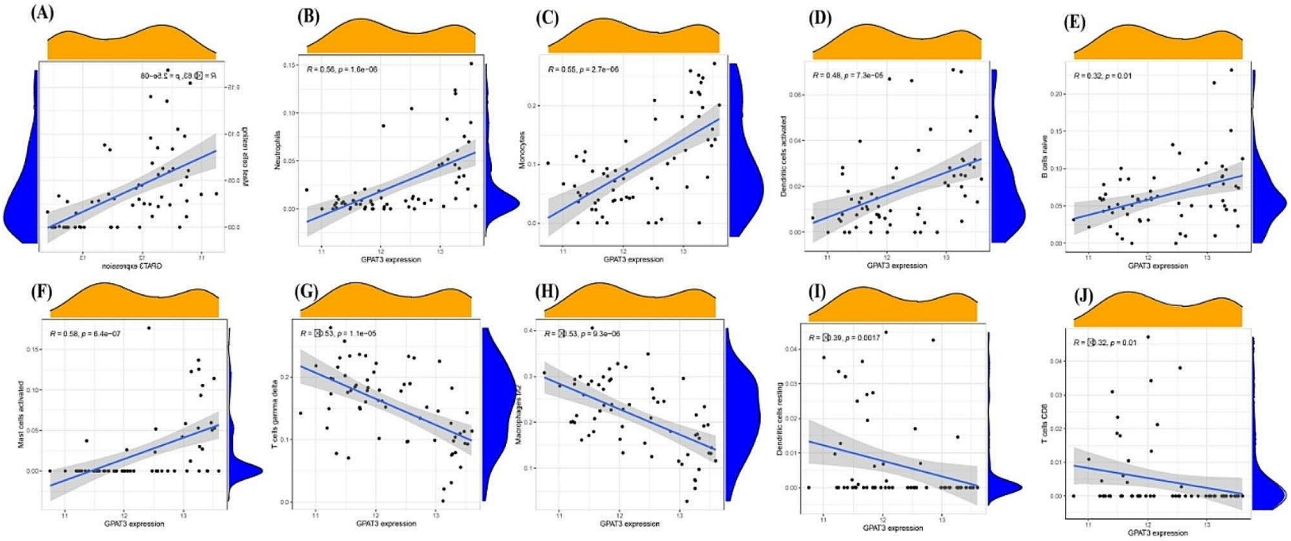

Fig. 6 Correlation between GPAT3 and infiltrating immune cells in NAFLD and healthy samples. (A. Mast cells resting), (B. Neutrophils), (C. Monocytes), (D. Dendritic cells activated), (E. B cells naive), (F. Mast cells activated), (G. T cells gamma delta), (H. Macrophages M2), (I. Dendritic cells resting), (J. T cells CD8)

dysregulation were obviously enriched. IL-17 is an inflammatory factor induced by Th17 cells, which can stimulate endothelial cells and epithelial cells to produce other inflammatory factors and chemokines, resulting in tissue damage. Overnutrition mediates DNA damage in hepatocytes through nonclassical prefoldin RPB5 interaction factor. DNA damage induces inflammation and neutrophilic infiltration of white adipose tissue through Th17 and IL-17 A, which in turn mediates insulin resistance and fatty acid release. Fatty acids are stored in the liver as triglycerides, leading to the development of NAFLD and NASH. TNF works through two receptors TNFR1 (also known as p55) and TNFR2 (also known as p75). TNFR1 is expressed in most tissues, and interacts with TNF, leading to a classic pro-inflammatory response, mostly through activation of the NF-κB and c-Jun pathways. Studies have that a high-fat diet increases the expression of TNF-a in the body, which further promotes the activation of NF-κB and TLRs signaling pathway, leading to the increase of inflammatory factors such as IL-6, and ultimately the formation of chronic inflammation. These results suggest that the selected DEGs are actively involved in the inflammatory process and are essential for the progression of NAFLD [36].

To identify potential diagnostic genes for NAFLD, two machine learning algorithms were used to analyze the 334 DEGs, thus four genes (*FOSB*, *GPAT3*, *RGCC*, and *RNF43*) were identified. FOSB is an early hepatocyte response protein that is essential for lipid metabolism [37]. Studies have shown that the expression of FOSB is

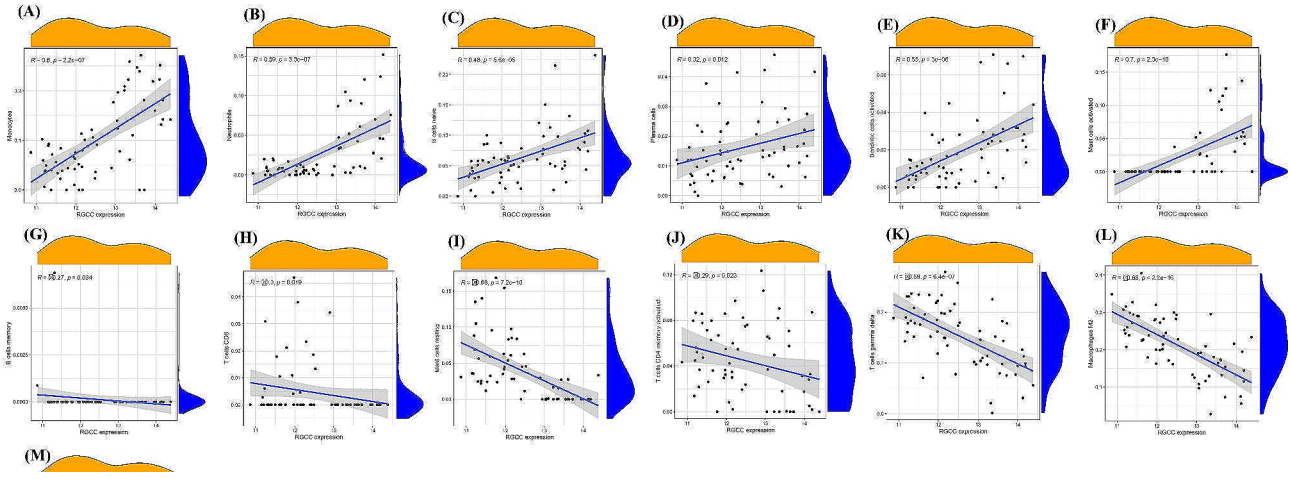

Fig. 7 Correlation between RGCC and infiltrating immune cells in NAFLD and healthy samples. (A. Monocytes), (B. Neutrophils), (C. B cells naive), (D. Plasma cells), (E. Dendritic cells activated), (F. Mast cells activated), (G. B cells memory), (H. T cells CD8), (I. Mast cells resting), (J. T cells CD4 memory activated), (K. T cells gamma delta), (L. Macrophages M2), (M. Dendritic cells resting)

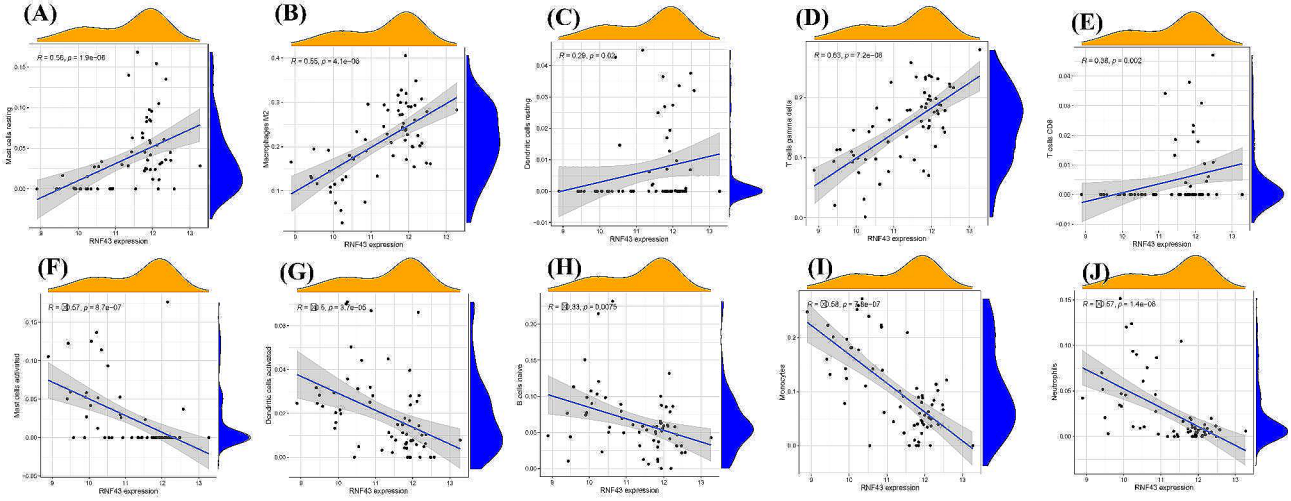

Fig. 8 Correlation between RNF43 and infiltrating immune cells in NAFLD and normal samples. (A. Mast cells resting), (B. Macrophages M2), (C. Dendritic cells resting), (D. T cells gamma delta), (E. T cells CD8), (F. Mast cells activated), (G. Dendritic cells activated), (H. B cells naive), (I. Monocytes), (J. Neutrophils)

significantly downregulated in patients with fatty liver disease [38]. Meanwhile, GPAT3 is the first critical rate-limiting enzyme in the glycerol-3-phosphate synthesis pathway [39]. Therefore, regulating the synthesis of triglycerides in the liver and reducing the accumulation of excess lipids in hepatocytes may be used as a novel therapeutic strategy to improve hepatic steatosis, and preventing and treating NAFLD [40]. Moreover, *RGCC*, also known as C13, is an important complement response gene that is widely expressed in various tissues [41]. It can regulate cell cycle, promote cell proliferation and differentiation [42], and regulate the immune response [43]. Interestingly, deletion or mutation of *RNF43* was found to lead to lipid accumulation and liver inflammation in non-obese mice fed a with normal diet. In humans, mutation of *RNF43* increases the risk of liver diseases such as fatty liver disease and liver cancer, as well as reduces the life expectancy of patients [44]. In addition, the ROC method confirmed their strong ability to differentiate NAFLD samples from normal samples. Thus, our findings suggest that *FOSB*, *GPAT3*, *RGCC*, and *RNF43* are potential diagnostic biomarkers for NAFLD.

We also examined *FOSB*, *GPAT3*, *RGCC*, and *RNF43* expression in patients with hepatitis B, hepatitis C, and AIH. There are some consistencies between the mouse liver transcriptome and the human blood transcriptome [45]. To compensate for the difficulty of obtaining human liver samples mouse liver could be used to detect the expression of some genes [46]. The results showed an increased expression of *FOSB* in patients with hepatitis B, an increased expression of *RNF43* in patients with hepatitis C, and an increased expression of *RNF43* along

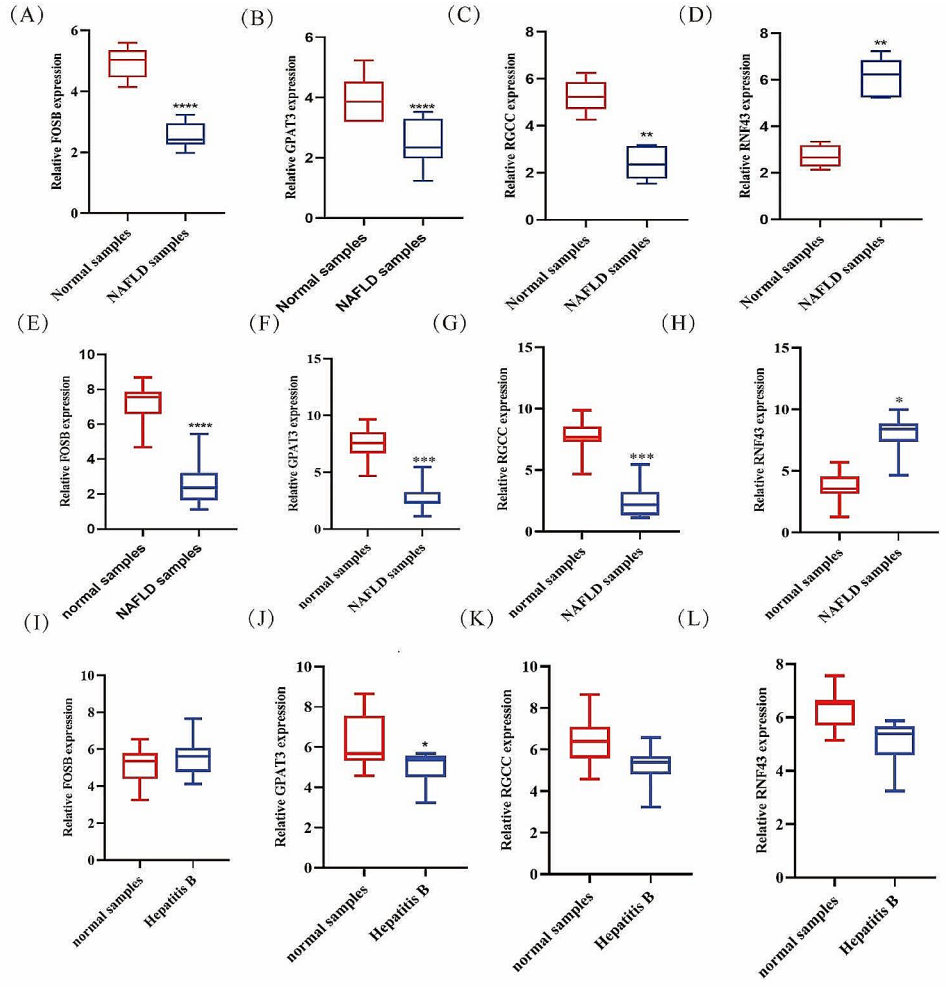

Fig. 9 mRNA levels of FOSB (**A**), GPAT3 (**B**), RGCC (**C**) and RNF43 (**D**) in NAFLD mice samples and normal control determined by RT-PCR. mRNA levels of FOSB (**E**-**H**), GPAT3 (**I**-**L**) in NAFLD human samples and normal samples from our cohort determined by RT-PCR

with a decreased expression of *RGCC* in patients with AIH. These results were consistent with the expression profile in patients with NAFLD. Many studies have suggested that *FOSB*, *RNF43* and *RGCC* are closely related to the inflammatory response of immune cells [47, 48]. Hepatitis B virus and hepatitis C virus infection can stimulate the inflammatory response of activated liver immune cells, thus change the expression of these genes will. However, hepatitis B, hepatitis C and AIH can only be diagnosed by the detection of corresponding virus genes and antibodies. In addition, FOSB is reported to be related to hepatitis C [49], while RNF43 and GPAT3 are related to hepatitis B [50, 51]. Our results show that in the diagnosis of NAFLD, the ROC value of the four gene expressions in blood is close to 1. It is suggested that the simultaneous changes of four genes are closely related to NAFLD. Therefore, combination of these four gene expressions in blood might be an alternative diagnostic method to the gold diagnostic standard (liver biopsy) with high sensitivity, specificity and safety.

Liver biopsy is the current gold standard for the diagnosis of NAFLD. Although it can directly observe the pathological features of the liver to diagnose NAFLD, it is inconvenient for patients to tolerate side effects such as pain and discomfort after puncture due to the trauma. Additionally, the technique of liver puncture biopsy is complicated, and many clinicians are not skilled enough resulting in dirty biopsy. However, for safety and financial cost, ultrasound which is the primary screening tool in clinical practice, is being used to diagnose NAFLD. Recently, a meta-analysis showed that the sensitivity of diagnosing moderate and severe fatty liver with ultrasound was 84.8% and the specificity was 93.6%. However, ultrasound has its drawbacks, its diagnostic sensitivity is only 55% when the fat content of the liver is below 20%. Although ultrasound screening for NAFLD is safer than liver tissue biopsy, it is not diagnostic of early NAFLD due to the clinician's experience. Our results show that the sensitivity of mRNA analysis using blood can reach a maximum of 0.985, thus reducing damage to the body.

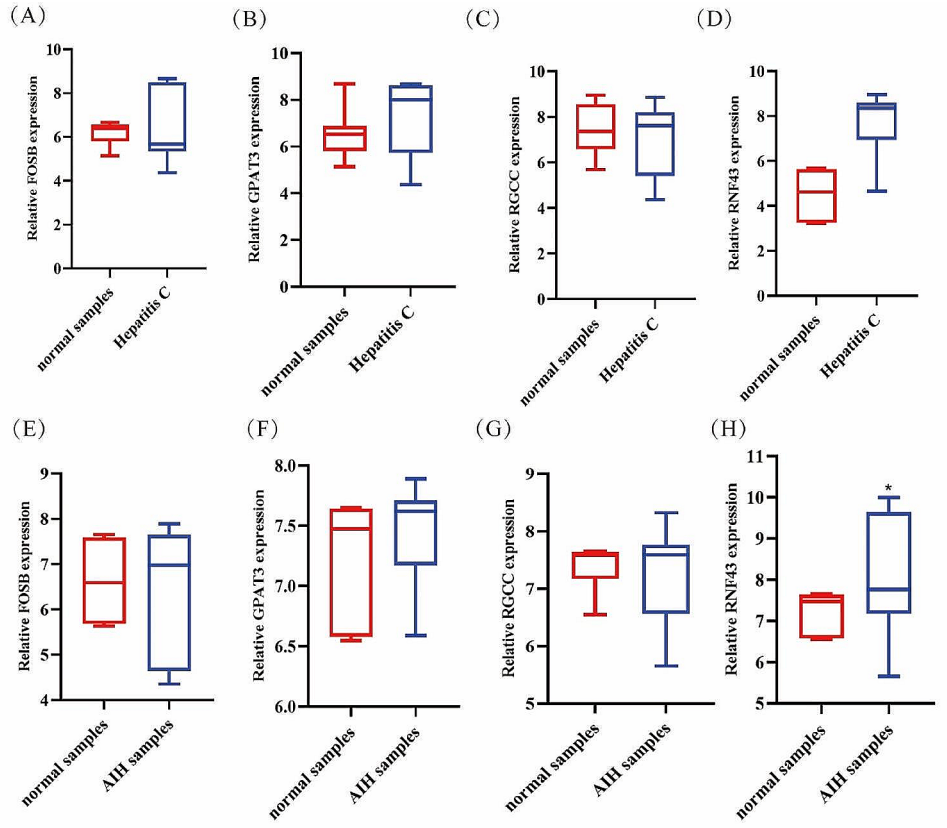

Fig. 10 mRNA levels of RGCC (**A**-**D**) and RNF43 (**E**-**H**) in NAFLD human samples and normal samples from our cohort determined by RT-PCR

We compared the expression of the genes in patients with hepatitis B, C, and autoimmune hepatitis and found that these genes were specifically expressed in patients with nonalcoholic fatty liver. Compared to biopsy, our diagnostic method is highly safe, which requires only a small amount of fingertip blood irrespective of the physician's skill. It is more acceptable to the patients as it is less harmful to the body. Compared to imaging, the diagnosis by finger blood is not influenced by the physician's experience and is more sensitive and specific for NAFLD.

In recent years, multiple studies have indicated that immune cell infiltration plays a crucial role in the occurrence and development of NAFLD. The progression of NAFLD is closely related to macrophages (Kupffer cells) [52], neutrophils [53], dendritic cells [54], and natural killer (NK) T cells [55]. Kupffer cells constitute about 20% of nonparenchymal hepatocytes and are involved in T lymphocyte activation and tolerance. Furthermore, TNF-α is mainly derived from Kupffer cells. In response to high-fat diet stimulation, the TNF-α levels are significantly increased in Kupffer cells, and large amounts of proinflammatory factors such as IL-6 are released to aggravate the inflammatory response [56]; additionally, stimuli such as a high-fat diet also increase the number of Kupffer cells themselves, thereby changing the activation state of NK T cells and inducing cell necrosis and apoptosis [57]. Moreover, increased oxidative stress activates Kupffer cells and the corresponding macrophages, and increases the levels of chemokines and cytokines [58]; thus, it plays a pivotal role in the progression of NAFLD. Therefore, it is necessary to evaluate the infiltration of immune cells and to identify the diversity of infiltrating immune cell components to reveal the molecular mechanisms in NAFLD to find new immunotherapeutic targets.

In this study, we observed dysregulated levels of $CD8^+$ T cells, resting dendritic cells, γδ T cells, M2 macrophages, resting mast cells, neutrophils, and naive B cells between normal and NAFLD samples. Moreover, the histamine produced during the degranulation of mast cells in the liver of patients with NAFLD induces an inflammatory response that damages the surrounding tissues. In livers from NAFLD mice, mast cells promote the progression of NAFLD to NASH hepatitis by upregulating the aldehydrogenase 1 family member A3 and downregulating microRNA-144-3. In contrast, mast-cell deficient mice exhibit improved the symptoms of NAFLD. The change of M1/M2 polarization may induce hepatic inflammation and hepatocyte injury, thus activating satellite cells. After activation, satellite cells release large numbers of collagen fibers, which promote liver fibrosis.

In addition, neutrophils [59], $CD4^+$ T cells [60], $CD8^+$ T cells [61], NK T cells [62], T helper 17 cells [63], and other immune cells have been confirmed to participate in the development of NAFLD. In the liver, these different types of cells regulate each other through the expression and release of inflammatory cytokines, chemokines, interleukins, and other cytokines in autocrine and paracrine modes, thus maintaining liver homeostasis. The abnormal expression of these secreted factors can cause necrosis and apoptosis of hepatocytes, activate satellite cells, and promote the development of NAFLD/NASH. Our data indicate that FOSB, GPAT3, RGCC, and RNF43 may participate in the progression of NAFLD by modulating some immune cells. Nevertheless, further studies are warranted to confirm these findings.

Conclusion

In this study, bioinformatics analysis indicates that *FOSB*, *GPAT3*, *RGCC*, and *RNF43* are the key DEGs for the comparison of NAFLD with healthy specimens. The results of this study provide novel insights into the potential molecular causality of NAFLD and potential therapeutic targets for NAFLD. Therefore, ongoing research focuses in refining the diagnostic value of existing biomarkers as well as discovering novel markers in the areas of epigenetics, transcriptomics and metabolomics, in the prospect of early reliable diagnosis that would guide targeted care.

Abbreviations

NAFLD	non-alcoholic fatty liver disease
GO	gene oncology
KEGG	Kyoto Encyclopedia of Genes and Genomes
LDL	low-density lipoprotein cholesterol
hPSC	human pluripotent stem cells
HCC	hepatocellular carcinoma
FGF	fibroblast growth factor
FGF21	Fibroblast growth factor 21

Supplementary Information

The online version contains supplementary material available at https://doi.org/10.1186/s12967-024-05315-3.

Supplementary Material 1

Supplementary Material 2

Acknowledgements

We thank the members of the Tianjin University of Traditional Chinese Medicine, Tianjin Medical University and Tianjin Second People's Hospital for valuable input. We acknowledge the Tianjin University of Traditional Chinese Medicine for assistance in generating RT-PCR data and instrumentation maintenance.

Author contributions

All authors contributed to the design of the study. JDW had primary responsibility for data curation, data analysis, writing up the manuscript, and is primary author of the manuscript. BTJ and JM designed the statistical analysis strategy and conducted the analyses. YHB and YGW acquired funding for study. YYW, LYG, FZ, SZL, KJN and WDL designed the statistical analysis strategy and conducted the analyses. DL, YW, LH, and YZ has directly accessed and verified the underlying data in the study. All authors read, edited, and approved the final version of the manuscript, and had final responsibility for the decision to submit for publication.

Funding

This work was supported by Major Science and Technology Project of Public Health in Tianjin (No. 21ZXGWSY00090), National Key R&D Program of China (2018YFC1706500).

Data availability

All data are available in the main text or the supplementary materials.

Declarations

Ethics approval and consent to participate

The study was reviewed and approved by Ethics Committee of Tianjin Second People's Hospital. All participants were fully informed about the study requirements and were required to accept the data sharing and privacy policy before participating in the study.

Consent for publication

No conflict of interest exits in the submission of this manuscript, and manuscript is approved by all authors for publication.

Conflict of interest

Authors declare that they have no competing interests.

Author details

[1]School of Integrative Medicine, Tianjin University of Traditional Chinese Medicine, Tianjin 301617, People's Republic of China
[2]Tianjin Second People's Hospital, Department of Integrated Traditional Chinese and Western Medicine, Tianjin 300192, People's Republic of China
[3]Public Health Science and Engineering College, Tianjin University of Traditional Chinese Medicine, Tianjin 301617, China
[4]School of Public Health, Tianjin Medical University, Tianjin 300070, China
[5]Department of General Surgery, Tianjin Medical University General Hospital, Tianjin 300052, China

Received: 7 December 2023 / Accepted: 20 May 2024
Published online: 04 July 2024

References

1. Powell EE, Wong VW, Rinella M. Non-alcoholic fatty liver disease. Lancet. 2021;397:2212–24.
2. Wong VW, Ekstedt M, Wong GL, Hagström H. Changing epidemiology, global trends and implications for outcomes of NAFLD. J Hepatol. 2023;79:842–52.
3. Zhou J, Zhou F, Wang W, Zhang XJ, Ji YX, Zhang P, She ZG, Zhu L, Cai J, Li H. Epidemiological features of NAFLD from 1999 to 2018 in China. Hepatology. 2020;71:1851–64.
4. Tilg H, Adolph TE, Dudek M, Knolle P. Non-alcoholic fatty liver disease: the interplay between metabolism, microbes and immunity. Nat Metab. 2021;3:1596–607.
5. Marengo A, Rosso C, Bugianesi E. Liver Cancer: connections with obesity, fatty liver, and cirrhosis. Annu Rev Med. 2016;67:103–17.
6. Targher G, Tilg H, Byrne CD. Non-alcoholic fatty liver disease: a multisystem disease requiring a multidisciplinary and holistic approach. Lancet Gastroenterol Hepatol. 2021;6:578–88.
7. Eng JM, Estall JL. Diet-Induced Models of Non-Alcoholic Fatty Liver Disease: Food for Thought on Sugar, Fat, and Cholesterol. *Cells* 2021, 10.
8. Polyzos SA, Kechagias S, Tsochatzis EA. Review article: non-alcoholic fatty liver disease and cardiovascular diseases: associations and treatment considerations. Aliment Pharmacol Ther. 2021;54:1013–25.
9. Vancells Lujan P, Viñas Esmel E, Sacanella Meseguer E. Overview of non-alcoholic fatty liver Disease (NAFLD) and the role of sugary food consumption and other Dietary Components in its development. Nutrients 2021, 13.
10. Lefebvre P, Staels B. Hepatic sexual dimorphism - implications for non-alcoholic fatty liver disease. Nat Rev Endocrinol. 2021;17:662–70.

11. Di Mauro S, Scamporrino A, Filippello A, Di Pino A, Scicali R, Malaguarnera R, Purrello F, Piro S. Clinical and molecular biomarkers for diagnosis and staging of NAFLD. Int J Mol Sci 2021, 22.
12. Chen H, Tan H, Wan J, Zeng Y, Wang J, Wang H, Lu X. PPAR-γ signaling in non-alcoholic fatty liver disease: Pathogenesis and therapeutic targets. Pharmacol Ther. 2023;245:108391.
13. Eftekhari A, Hasanzadeh A, Khalilov R, Hosainzadegan H, Ahmadian E, Eghbal MA. Hepatoprotective role of berberine against paraquat-induced liver toxicity in rat. Environ Sci Pollut Res Int. 2020;27:4969–75.
14. Serra-Burriel M, Juanola A, Serra-Burriel F, Thiele M, Graupera I, Pose E, Pera G, Grgurevic I, Caballeria L, Piano S, et al. Development, validation, and prognostic evaluation of a risk score for long-term liver-related outcomes in the general population: a multicohort study. Lancet. 2023;402:988–96.
15. Baran A, Keskin C, Baran MF, Huseynova I, Khalilov R, Eftekhari A, Irtegun-Kandemir S, Kavak DE. Ecofriendly Synthesis of Silver Nanoparticles Using Ananas comosus Fruit Peels: Anticancer and Antimicrobial Activities. *Bioinorg Chem Appl* 2021, 2021:2058149.
16. Rinella ME, Terrault N, Neuschwander-Tetri B, Loomba R, Abdelmalek M. Reply: ELF in the risk stratification of NAFLD-Are the ELF thresholds suggested by the AASLD guidelines appropriate? Hepatology. 2023;78:E103–4.
17. Baran A, Fırat Baran M, Keskin C, Hatipoğlu A, Yavuz Ö, İrtegün Kandemir S, Adican MT, Khalilov R, Mammadova A, Ahmadian E, et al. Investigation of Antimicrobial and Cytotoxic properties and specification of silver nanoparticles (AgNPs) derived from Cicer arietinum L. Green Leaf Extract. Front Bioeng Biotechnol. 2022;10:855136.
18. Gunashova GY, SYNTHESIS OF SILVER, NANOPARTICLES USING A THERMOPHILIC BACTERIUM STRAIN ISOLATED FROM, THE SPRING YUKHARI ISTISU OF THE KALBAJAR REGION (AZERBAIJAN). Adv Biology Earth Sci. 2022;7:198–204.
19. Wang Y, Chen G, Shao W. Identification of ferroptosis-related genes in Alzheimer's Disease Based on Bioinformatic Analysis. Front Neurosci. 2022;16:823741.
20. Flippo KH, Trammell SAJ, Gillum MP, Aklan I, Perez MB, Yavuz Y, Smith NK, Jensen-Cody SO, Zhou B, Claflin KE, et al. FGF21 suppresses alcohol consumption through an amygdalo-striatal circuit. Cell Metab. 2022;34:317–e328316.
21. Katsumura S, Siddiqui N, Goldsmith MR, Cheah JH, Fujikawa T, Minegishi G, Yamagata A, Yabuki Y, Kobayashi K, Shirouzu M, et al. Deadenylase-dependent mRNA decay of GDF15 and FGF21 orchestrates food intake and energy expenditure. Cell Metab. 2022;34:564–e580568.
22. Ahuja P, Bi X, Ng CF, Tse MCL, Hang M, Pang BPS, Iu ECY, Chan WS, Ooi XC, Sun A, et al. Src homology 3 domain binding kinase 1 protects against hepatic steatosis and insulin resistance through the Nur77-FGF21 pathway. Hepatology. 2023;77:213–29.
23. Aguilera MO, Robledo E, Melani M, Wappner P, Colombo MI. FKBP8 is a novel molecule that participates in the regulation of the autophagic pathway. Biochim Biophys Acta Mol Cell Res. 2022;1869:119212.
24. Xie Z, Li EW, Gao G, Du Y, Wang M, Wang H, Wang P, Qiao Y, Su Y, Xu J, et al. Zexie Tang targeting FKBP38/mTOR/SREBPs pathway improves hyperlipidemia. J Ethnopharmacol. 2022;290:115101.
25. Gao P, Wang H, Li H, Shu L, Han Z, Li S, Cheng H, Dai X. Mir-21-5p inhibits the Proliferation, Migration, and Invasion of Glioma by Targeting S100A10. J Cancer. 2023;14:1781–93.
26. Li H, Dai X, Zhou L, Nie J, Cheng H, Gao P. Ferroptosis-related gene MTF-1 as a novel prognostic biomarker in low-grade glioma and its correlation with immune infiltration. Heliyon. 2023;9:e21159.
27. Fan Y, Dong W, Wang Y, Zhu S, Chai R, Xu Z, Zhang X, Yan Y, Yang L, Bian Y. Glycyrrhetinic acid regulates impaired macrophage autophagic flux in the treatment of non-alcoholic fatty liver disease. Front Immunol. 2022;13:959495.
28. Greener JG, Kandathil SM, Moffat L, Jones DT. A guide to machine learning for biologists. Nat Rev Mol Cell Biol. 2022;23:40–55.
29. Do MH, Lee HHL, Lee JE, Park M, Oh MJ, Lee HB, Park JH, Jhun H, Kim JH, Kang CH, Park HY. Gellan gum prevents non-alcoholic fatty liver disease by modulating the gut microbiota and metabolites. Food Chem. 2023;400:134038.
30. Sheka AC, Adeyi O, Thompson J, Hameed B, Crawford PA, Ikramuddin S. Nonalcoholic steatohepatitis: a review. JAMA. 2020;323:1175–83.
31. Zhang X, Coker OO, Chu ES, Fu K, Lau HCH, Wang YX, Chan AWH, Wei H, Yang X, Sung JJY, Yu J. Dietary cholesterol drives fatty liver-associated liver cancer by modulating gut microbiota and metabolites. Gut. 2021;70:761–74.
32. Sowah LA, Smeaton L, Brates I, Bhattacharya D, Linas B, Kreter B, Wagner-Cardoso S, Solomon S, Sulkowski M, Robbins GK. Perspectives on Adherence from the ACTG 5360 MINMON Trial: a Minimum Monitoring Approach with 12 weeks of Sofosbuvir/Velpatasvir in Chronic Hepatitis C treatment. Clin Infect Dis. 2023;76:1959–68.
33. Kim SK, Fujii T, Kim SR, Nakai A, Lim YS, Hagiwara S, Kudo M. Hepatitis B Virus Treatment and Hepatocellular Carcinoma: controversies and approaches to Consensus. Liver Cancer. 2022;11:497–510.
34. Park J, Le AK, Tseng TC, Yeh ML, Jun DW, Trinh H, Wong GLH, Chen CH, Peng CY, Kim SE, et al. Progression rates by Age, Sex, Treatment, and Disease Activity by AASLD and EASL Criteria: data for Precision Medicine. Clin Gastroenterol Hepatol. 2022;20:874–e885874.
35. Ye Q, Kam LY, Yeo YH, Dang N, Huang DQ, Cheung R, Nguyen MH. Substantial gaps in evaluation and treatment of patients with hepatitis B in the US. J Hepatol. 2022;76:63–74.
36. Wang C, Li Z, Liu Y, Yuan L. Exosomes in atherosclerosis: performers, bystanders, biomarkers, and therapeutic targets. Theranostics. 2021;11:3996–4010.
37. Shi F, Zi Y, Lu Z, Li F, Yang M, Zhan F, Li Y, Li J, Zhao L, Lin L, Qin Z. Bacillus subtilis H2 modulates immune response, fat metabolism and bacterial flora in the gut of grass carp (Ctenopharyngodon Idellus). Fish Shellfish Immunol. 2020;106:8–20.
38. Gao S, Gang J, Yu M, Xin G, Tan H. Computational analysis for identification of early diagnostic biomarkers and prognostic biomarkers of liver cancer based on GEO and TCGA databases and studies on pathways and biological functions affecting the survival time of liver cancer. BMC Cancer. 2021;21:791.
39. Gao M, Liu L, Wang X, Mak HY, Liu G, Yang H. GPAT3 deficiency alleviates insulin resistance and hepatic steatosis in a mouse model of severe congenital generalized lipodystrophy. Hum Mol Genet. 2020;29:432–43.
40. Sim MFM, Persiani E, Talukder MMU, McIlroy GD, Roumane A, Edwardson JM, Rochford JJ. Oligomers of the lipodystrophy protein seipin may co-ordinate GPAT3 and AGPAT2 enzymes to facilitate adipocyte differentiation. Sci Rep. 2020;10:3259.
41. Guo Z, Chen M, Chao Y, Cai C, Liu L, Zhao L, Li L, Bai QR, Xu Y, Niu W, et al. RGCC balances self-renewal and neuronal differentiation of neural stem cells in the developing mammalian neocortex. EMBO Rep. 2021;22:e51781.
42. Qin Z, Wang W, Liao D, Wu X, Li X. UPLC-Q/TOF-MS-Based serum Metabolomics reveals hypoglycemic effects of Rehmannia Glutinosa, Coptis chinensis and their combination on High-Fat-Diet-Induced diabetes in KK-Ay mice. Int J Mol Sci 2018, 19.
43. Cui XB, Luan JN, Dong K, Chen S, Wang Y, Watford WT, Chen SY. RGC-32 (response gene to complement 32) Deficiency protects endothelial cells from inflammation and attenuates atherosclerosis. Arterioscler Thromb Vasc Biol. 2018;38:e36–47.
44. Belenguer G, Mastrogiovanni G, Pacini C, Hall Z, Dowbaj AM, Arnes-Benito R, Sljukic A, Prior N, Kakava S, Bradshaw CR, et al. RNF43/ZNRF3 loss predisposes to hepatocellular-carcinoma by impairing liver regeneration and altering the liver lipid metabolic ground-state. Nat Commun. 2022;13:334.
45. Liu K, Yang L, Wang G, Liu J, Zhao X, Wang Y, Li J, Yang J. Metabolic stress drives sympathetic neuropathy within the liver. Cell Metab. 2021;33:666–e675664.
46. Wang L, Cheng B, Ju Q, Sun BK. AhR regulates Peptidoglycan-Induced Inflammatory Gene expression in human keratinocytes. J Innate Immun. 2022;14:124–34.
47. Mostafa MM, Rider CF, Shah S, Traves SL, Gordon PMK, Miller-Larsson A, Leigh R, Newton R. Glucocorticoid-driven transcriptomes in human airway epithelial cells: commonalities, differences and functional insight from cell lines and primary cells. BMC Med Genomics. 2019;12:29.
48. Metidji A, Omenetti S, Crotta S, Li Y, Nye E, Ross E, Li V, Maradana MR, Schiering C, Stockinger B. The Environmental Sensor AHR protects from inflammatory damage by maintaining Intestinal Stem Cell Homeostasis and Barrier Integrity. Immunity. 2018;49:353–e362355.
49. Lupberger J, Croonenborghs T, Roca Suarez AA, Van Renne N, Jühling F, Oudot MA, Virzì A, Bandiera S, Jamey C, Meszaros G, et al. Combined analysis of Metabolomes, proteomes, and transcriptomes of Hepatitis C virus-infected cells and liver to identify pathways Associated with Disease Development. Gastroenterology. 2019;157:537–e551539.
50. Katoh M. Multi–layered prevention and treatment of chronic inflammation, organ fibrosis and cancer associated with canonical WNT/β–catenin signaling activation (review). Int J Mol Med. 2018;42:713–25.
51. Chen S, Huang Y, Su H, Zhu W, Wei Y, Long Y, Shi Y, Wei J. The Integrated Analysis of Transcriptomics and Metabolomics unveils the Therapeutical Effect of Asiatic Acid on Alcoholic Hepatitis in rats. Inflammation. 2022;45:1780–99.
52. Blériot C, Barreby E, Dunsmore G, Ballaire R, Chakarov S, Ficht X, De Simone G, Andreata F, Fumagalli V, Guo W, et al. A subset of Kupffer

cells regulates metabolism through the expression of CD36. Immunity. 2021;54:2101–e21162106.
53. Jackson-Jones LH, Smith P, Portman JR, Magalhaes MS, Mylonas KJ, Vermeren MM, Nixon M, Henderson BEP, Dobie R, Vermeren S, et al. Stromal cells Covering Omental Fat-Associated lymphoid clusters trigger formation of Neutrophil aggregates to capture peritoneal contaminants. Immunity. 2020;52:700–e715706.
54. Brenner C, Galluzzi L, Kepp O, Kroemer G. Decoding cell death signals in liver inflammation. J Hepatol. 2013;59:583–94.
55. Adachi Y, Ueda K, Nomura S, Ito K, Katoh M, Katagiri M, Yamada S, Hashimoto M, Zhai B, Numata G, et al. Beiging of perivascular adipose tissue regulates its inflammation and vascular remodeling. Nat Commun. 2022;13:5117.
56. Yu Y, Liu Y, An W, Song J, Zhang Y, Zhao X. STING-mediated inflammation in Kupffer cells contributes to progression of nonalcoholic steatohepatitis. J Clin Invest. 2019;129:546–55.
57. Wan J, Benkdane M, Teixeira-Clerc F, Bonnafous S, Louvet A, Lafdil F, Pecker F, Tran A, Gual P, Mallat A, et al. M2 kupffer cells promote M1 Kupffer cell apoptosis: a protective mechanism against alcoholic and nonalcoholic fatty liver disease. Hepatology. 2014;59:130–42.
58. Feng Y, Dong H, Sun B, Hu Y, Yang Y, Jia Y, Jia L, Zhong X, Zhao R. METTL3/METTL14 transactivation and m(6)A-Dependent TGF-β1 translation in activated Kupffer cells. Cell Mol Gastroenterol Hepatol. 2021;12:839–56.
59. van der Windt DJ, Sud V, Zhang H, Varley PR, Goswami J, Yazdani HO, Tohme S, Loughran P, O'Doherty RM, Minervini MI, et al. Neutrophil extracellular traps promote inflammation and development of hepatocellular carcinoma in nonalcoholic steatohepatitis. Hepatology. 2018;68:1347–60.
60. Wang H, Zhang H, Wang Y, Brown ZJ, Xia Y, Huang Z, Shen C, Hu Z, Beane J, Ansa-Addo EA, et al. Regulatory T-cell and neutrophil extracellular trap interaction contributes to carcinogenesis in non-alcoholic steatohepatitis. J Hepatol. 2021;75:1271–83.
61. Wolf MJ, Adili A, Piotrowitz K, Abdullah Z, Boege Y, Stemmer K, Ringelhan M, Simonavicius N, Egger M, Wohlleber D, et al. Metabolic activation of intrahepatic CD8 + T cells and NKT cells causes nonalcoholic steatohepatitis and liver cancer via cross-talk with hepatocytes. Cancer Cell. 2014;26:549–64.
62. Cho DS, Schmitt RE, Dasgupta A, Ducharme AM, Doles JD. Single-cell deconstruction of post-sepsis skeletal muscle and adipose tissue microenvironments. J Cachexia Sarcopenia Muscle. 2020;11:1351–63.
63. Kawano Y, Edwards M, Huang Y, Bilate AM, Araujo LP, Tanoue T, Atarashi K, Ladinsky MS, Reiner SL, Wang HH, et al. Microbiota imbalance induced by dietary sugar disrupts immune-mediated protection from metabolic syndrome. Cell. 2022;185:3501–e35193520.

Publisher's Note